2002

The Influence of Open Versus Periodic Alongshore Boundaries on Circulation Near Submarine Canyons

Michael S. Dinniman
Old Dominion University, msd@ccpo.odu.edu

John M. Klinck
Old Dominion University, jklinck@odu.edu

NOTES AND CORRESPONDENCE

The Influence of Open versus Periodic Alongshore Boundaries on Circulation near Submarine Canyons

MICHAEL S. DINNIMAN AND JOHN M. KLINCK

Center for Coastal Physical Oceanography, Old Dominion University, Norfolk, Virginia

7 March 2001 and 22 April 2002

ABSTRACT

It is impractical to create gridded numerical models of coastal circulation with sufficient resolution around small topographic features, such as submarine canyons, and still have the alongshore boundaries placed beyond the decay distance of coastal trapped waves. Two solutions to this problem are to make the alongshore boundaries either open or periodic. Numerical simulations were performed with upwelling and downwelling winds to compare the effects of these different choices for boundary conditions.

Several open boundary formulations were tried and three are discussed in detail. The offshore boundary was specified as ''no gradient'' for all variables with no serious effect. The ''modified'' Orlanski radiation condition is used for all variables at the alongshore boundaries, except the vertically integrated flow that has the strongest effect on the model solution.

An alongshore pressure gradient, opposing the wind, develops in the model if the modified Orlanski radiation condition is applied to the barotropic flow, causing slower currents near the surface and deep undercurrents away from the shelf. The other cases, which combined either a radiation or a relaxation boundary condition with a local solution of the barotropic equations on the boundary, were at least initially similar to the periodic case but with slower alongshore flow. The initial impact of these differences on the circulation within the canyon was small. The models with the open boundaries were more stable (did not develop strong flow meanders) than the cases with periodic conditions as initial transients are not trapped, and amplified, within the domain. Thus, open cases, especially with the upwelling winds, could run for extended times.

1. Introduction

Submarine canyons along continental shelf edges are important topographical features that can have large impacts on coastal processes (Hickey 1995). Many recent numerical simulations (e.g., She and Klinck 2000; Ardhuin et al. 1999; Haidvogel and Beckmann 1998; Pérenne et al. 1997; Allen 1996; Klinck 1996) reveal some physical insight into how these features affect ocean circulation. One problem with all these simulations, however, is that, for a finite-difference numerical model, it is usually impractical to create a model grid with sufficient resolution around the canyon ($\leq$1 km) yet with the alongshore dimension large enough to account for all areas that influence the circulation around the canyon. That would require placing the boundaries far enough away to cover the decay distance of coastal trapped waves, perhaps 1000 km in the direction of phase propagation (Huthnance 1992). The most common solutions to this problem are to make the alongshore boundaries either open or periodic.

Each of these boundary conditions has its own problems. Disturbances created in a periodic domain cannot advect or propagate out of the model, which can lead to rapid accumulation of energy and model instability. Also, alongshore pressure gradients cannot be naturally created in a periodic model (although they can be externally imposed), which limits the realism of the flow. On the other hand, it has been shown that open boundary conditions (OBCs) on the hydrostatic primitive equations are an ill-posed problem (Oliger and Sündstrom 1978; Bennett and Kloeden 1978) in that a small change in the OBC can result in a large change in the interior solution. Many studies have been published using different ''passive'' (where the exterior solution is not known and the boundary condition must be assumed or derived from the interior solution) OBCs. However, the ill-posedness of the problem usually means that what works for one particular model setup will not be the best solution for another setup. Most studies of different passive OBCs used two-dimensional linear or nonlinear models (Chapman 1985; Røed and Cooper 1987; Palma

Corresponding author address: Mr. Michael S. Dinniman, Center for Coastal Physical Oceanography, Old Dominion University, Norfolk, VA 23529.
E-mail: msd@ccpo.odu.edu

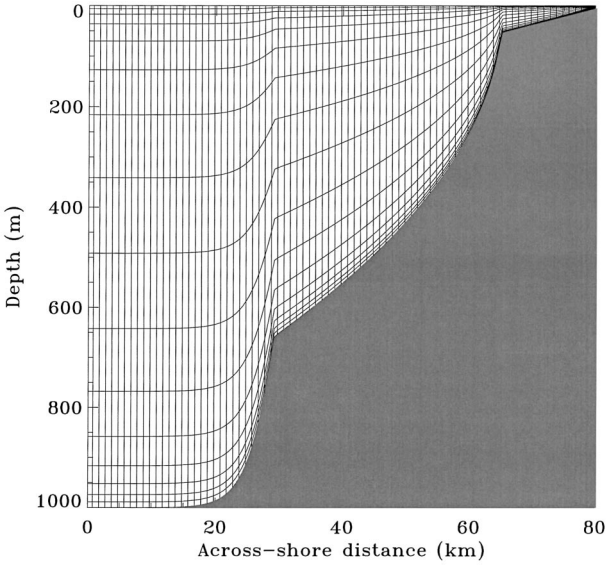

FIG. 1. Across-shore model bathymetry and layer thickness along the canyon axis.

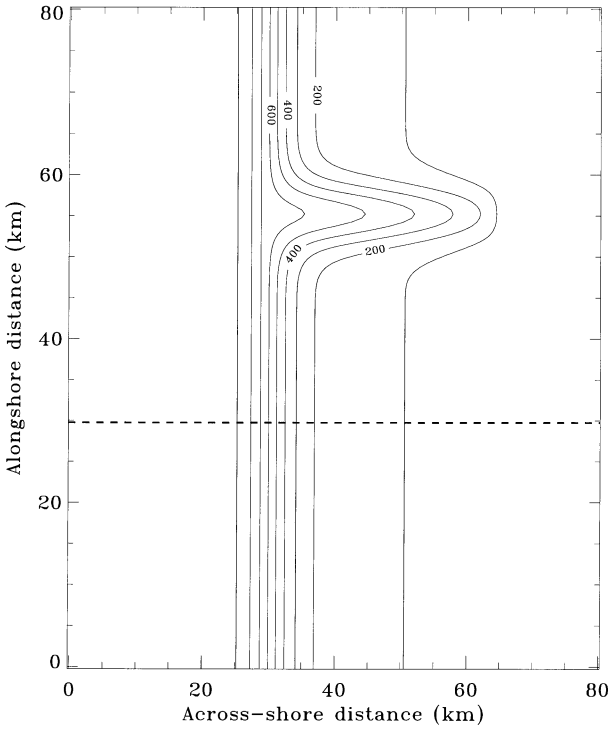

FIG. 2. Model bathymetry. The contour depths are in m. The heavy dashed line represents the section across which transports will be calculated (Figs. 4 and 10).

and Matano 1998) although there have been a few recent studies that use barotropic models (Jensen 1998; Palma and Matano 2000). This paper is not meant to be a comparison of all possible OBCs but instead is derived from our attempts to find a simple-to-implement OBC to use in our numerical studies of canyon circulation when there are few or no observations of the flow outside the immediate vicinity of the canyon.

For this paper, a model domain representative of a generic submarine canyon in a continental shelf off the U.S. West Coast was created and the vertically stratified ocean was forced with a constant alongshore wind stress. Simulations were created using different combinations of open or periodic boundary conditions forced by upwelling (southward for this geometry) or downwelling winds. The next section describes the model setup. The simulations are then compared and discussed and conclusions are drawn about these different boundary conditions.

2. Model configuration

The Rutgers/UCLA Regional Ocean Model System (ROMS) [version 1.0(beta)] developed by Hernan Arango and Alexander Shchepetkin was used for this study. ROMS is a coarse-grain parallel primitive equation ocean circulation model derived from the serial S-coordinate Rutgers University Model (SCRUM, see Hedström 1997). The model has a free surface and uses a vertical *s* (terrain following) coordinate well suited for domains with variable bathymetry.

The model domain was 80 km in the alongshore and across-shore directions with a horizontal resolution of 500 m in each dimension. The 16 vertical levels were placed so that they were concentrated toward the top and bottom of the model domain (Fig. 1). The bathymetry consisted of a generic continental slope/shelf with a shelf depth ranging from 5 m at the coast to 150 m at the shelf break and an abyssal depth of 1000 m with a single straight canyon cut into the shelf (Fig. 2). The geometry of the canyon was chosen to be similar to (although somewhat wider than) that of Astoria Canyon, which is located off the U.S. West Coast just offshore of the mouth of the Columbia River: axial bottom depth (H) = 600 m, depth of the shelf break (H_S) = 150 m, half-width at midcanyon ($W/2$) = 4 km, and length (L) = 23 km. However, our canyon was not nearly as steep (maximum slope $\approx 5°$) as Astoria where the maximum slope approaches 45° in some places (Hickey 1997). This reduction avoids some of the problems with artificial pressure gradients that occur with steep bathymetry and terrain-following coordinate systems. An f-plane approximation was made so as to avoid the problem of a mismatch in the Coriolis parameter at a periodic boundary; the chosen value ($f = 1.053 \times 10^{-4}$ s^{-1}) matches that near Astoria Canyon. The canyon was intentionally placed farther away from the southern boundary because the greatest difficulties with the open boundaries occurred with the ''upstream'' (southern) boundary when upwelling (southward) winds were used. Upstream here refers to the direction of phase propagation of coastal trapped waves (CTWs), which is cyclonic around the ocean (northward for this geometry)

in the absence of any mean flow (Huthnance et al. 1986; Csanady 1988).

The simulation used both temperature and salinity, and the density was computed using a nonlinear equation of state. The Laplacian horizontal mixing was along geopotential surfaces with coefficients of 10 $m^2\ s^{-1}$ and 5 $m^2\ s^{-1}$ for momentum and tracers, respectively. Vertical mixing of momentum and tracers used the ''K profile parameterization'' mixing scheme (Large et al. 1994). The vertical flux for both heat and freshwater was set to zero at the top and bottom surfaces. Quadratic bottom stress, with a coefficient of 3.0×10^{-3} (nondimensional), was applied as a body force over the bottom layer.

The initial vertical stratification for all the simulations was an analytical approximation to hydrographic data obtained near Astoria Canyon in the spring of 1983 (Reed 1984). As this was an El Niño year and the upper water column off the U.S. West Coast was substantially warmer than usual (Cannon et al. 1985), the water was strongly stratified. The internal radius of deformation estimated as $\lambda = NH/f$, where $N^2 = -g\Delta\rho/\rho_0 H$ is the square of the buoyancy frequency, is 48.8 km for $H =$ 600 m, which is comparable to similar calculations around Astoria (Hickey 1997). A second estimate calculated as $\lambda = c/f$, where c is the internal gravity wave speed computed using a dynamical mode calculation (Wilkin 1987), is 10.2 km for $H = 150$ m and 14.9 km for $H = 900$ m. In either case, the simulated canyon can be considered ''narrow'' since the internal radius of deformation is greater than the canyon width (Klinck 1988).

At the start of the simulation the flow was zero and the free surface and isopycnals were level. Eight simulations were run: four with upwelling wind stress (periodic alongshore boundaries and three different open boundaries) and four with downwelling wind stress. In each case, the wind stress was in the alongshore direction only and was ramped up to its maximum magnitude of 0.05 N m^{-2} over 2 days and then held constant over the duration of the experiment. There was no spatial variability in the wind at any time. The wind forcing was applied as a body force over the top three layers of the domain, ranging in depth from 1 m up against the coast to 36 m over the abyssal plain.

The OBCs on the north and south ends of the domain had the strongest effect on the solutions. First, the constant wind forcing through both open boundaries has often been shown to create problems in a coastal model even with constant alongshore bathymetry (e.g., Chapman 1985; Palma and Matano 1998, 2000). Second, as shown by running some of the experiments with and without a canyon, the variation in the bathymetry did cause meridional variations in the circulation that affected the stability of the simulation. Finally, since we did not want to assume any solution ''far'' from the canyon that was not at least partially derived from the interior solution, we did not use any of the methods commonly invoked on open boundaries to push the model toward a specific state (e.g., imposing a velocity at the boundaries; relaxation to a given velocity, surface height, temperature or salinity profile, etc.). Instead, several passive techniques were implemented on the northern and southern boundaries. Separate boundary conditions were computed for the barotropic (depth-averaged) velocities, the baroclinic velocities, the free surface height, and the temperature and salinity. The boundary conditions for the two-dimensional flow had the strongest effect on the structure and variability of the solutions.

Most of the methods we tried were different solutions to the Sommerfeld radiation condition applied to a given quantity Φ:

$$\Phi_t \pm C\Phi_y = 0,$$

where the upper sign is used at the north open boundary and the lower sign is used at the south. Differences among the various methods are in the choice of the phase speed C. Several methods led to solutions that were clearly unstable for our experiment, including a two-dimensional upstream radiation scheme (Raymond and Kuo 1984), gravity wave radiation ($C =$ speed of external gravity waves), and zero gradient conditions ($C = \infty$). Between the Orlanski (1976) and ''modified'' Orlanski (MO, Camerlengo and O'Brien 1980) radiation schemes, the MO method worked the best and is one of the three solutions we will discuss. In the Orlanski method, the phase speed C is computed from interior values of the quantity and is simply $C = -\Phi_t/\Phi_y$ if an outgoing wave through the boundary is indicated ($\mp\Phi_t/\Phi_y > 0$), otherwise $C = 0$. The modified Orlanski scheme forces the phase speed to be either the maximum limit as defined by the model grid spacing and time step ($C = \Delta y/\Delta t$) or zero. The MO method was used on the north and south boundaries for the free surface height, baroclinic velocities, and temperature and salinity in all three of the open boundary solutions that we will compare. For the MO test case, this solution was also used on both components of the barotropic flow.

Røed and Smedstad (1984) suggested separating the depth averaged flow into ''free'' and ''forced'' components and using a radiation scheme of some sort on the free component only. The forced mode, or local, solution does not require an open boundary condition since it uses a linear subset of the governing equations with no normal derivatives and is calculated as

$$\frac{\partial(UD)}{\partial t} = fVD - gD\frac{\partial \eta}{\partial x} - \tau_{bx} + \tau^{sx}$$

$$\frac{\partial(VD)}{\partial t} = -fUD - \tau_{by} + \tau^{sy}$$

$$\frac{\partial \eta}{\partial t} = -\frac{\partial(UD)}{\partial x},$$

where U and V are the zonal and meridional vertically

averaged velocities, D is the depth, f is the Coriolis parameter, g is the local acceleration due to gravity, η is the surface height, τ_b is the bottom friction, and τ^s is the wind stress. The free mode is then computed by subtracting the forced mode from the total solution. For one of the original test cases, we applied the modified Orlanski condition to the free part of the normal component of the barotropic velocity at the northern and southern boundaries. This worked well with the original bathymetry, but when the model depth at the coast was reduced from 50 to 5 m, this condition became unstable for upwelling winds near the end of the 20-day simulation. Other simulations with a more realistic topography using this boundary condition also proved to be unstable (and would only run for a few days) and thus we removed this condition from consideration.

Another open boundary condition was the Flather radiation scheme (Flather 1976) applied to the free component of the barotropic flow as proposed by Palma and Matano (1998, 2000). The Flather technique (henceforth referred to as FLR) combines the Sommerfeld radiation condition with a one-dimensional version of the continuity equation as

$$U = U_0(t) \pm \frac{C}{D}[\eta - \eta_0(t)],$$

where U_0 and η_0 are specified values. Since we are not prescribing the velocity or the height on the boundary, we will set them to zero (for the free solution) and allow the differences to radiate at the speed of external gravity waves. This leads to

$$U = \pm\sqrt{\frac{g}{D}}\eta$$

being applied to the free part of the normal component of the barotropic velocity at the northern and southern boundaries.

The final open boundary condition did not use a radiative boundary condition but instead used the flow relaxation scheme of Martinsen and Engedahl (1987). Within an area close to the open boundary, a quantity is relaxed to a given solution by

$$\Phi = \alpha(y)\Phi_{\text{pre}} + (1 - \alpha(y))\Phi_{\text{int}},$$

where Φ_{pre} is the prescribed solution, Φ_{int} is the calculated interior solution, $\alpha(y)$ is some smoothly varying function ranging from 1 at the boundary to 0 at some interior point, and Φ is the new updated value. For our simulations, we used $\alpha(y) = 1 - \tanh(0.5J)$, where J is the number of points away from the boundary (from 0 to 10). Palma and Matano (1998, 2000) also suggested using this technique with the local solution as the prescribed value on the boundary. We ran a case (henceforth referred to as FRS) with this specification of the normal component of the barotropic velocity at the northern and southern boundaries.

In all the simulations (open and periodic alongshore boundaries), the offshore boundary was open with no cross-boundary gradients and the coastal (eastern) boundary was closed with a free-slip condition. No global constraints on the volume were imposed, and the total water flux into or out of the domain was allowed to be nonzero.

Aside on sponges at open boundaries

One particular problem that we had with the simulation deals with the use of a sponge (enhanced dissipation) over a region near the open boundaries. It was originally thought to be necessary to increase the horizontal mixing coefficients to prevent noise generated at the boundaries from affecting the entire domain over long integrations. The sponge was not applied to the alongshore component of velocity as it seemed important not to restrict the alongshore flow (see Chapman 1985).

A problem occurs where the sponge intersects the steep topography (the continental slope continued through both open boundaries). Errors in computing the horizontal tracer gradients over the steep bathymetry (Laplacian mixing was along geopotential surfaces) initially led to horizontal mixing in the cross-shelf direction. Along the edge of the sponge, the difference in mixing coefficients causes differences in the density in the alongshore direction, which leads to erroneous currents. This is shown most clearly in one experiment without wind stress, nonlinear momentum advection terms, Coriolis terms, and vertical mixing. With no wind and a horizontally uniform initial density distribution, there should be no flow in the model. However, artificial pressure gradients, resulting from the combination of vertical stratification and a terrain-following coordinate system, force a weak circulation over much of the domain. Boundary sponges create an additional flow toward the interior along the continental slope at both open boundaries (Fig. 3).

In simulations with complete dynamics, the boundary sponge creates flow along the steepest part of the continental slope, which affects deep flow in the canyon. In some parts of the model domain where the forced flow is weak, a small but noticeable effect on the circulation occurs (mostly differences in the circulation along the shelf and in the mouth of the canyon). Because of this, we did not use the sponge since the model would run for a long integration ($>$30 days) without it.

3. Results

Simulations lasting 20 model days were run for each boundary condition for upwelling and downwelling winds (eight total). For each wind direction, comparisons were made between the periodic boundary case and the three open boundary (MO, FLR, and FRS) simulations. The total alongshore volume transport over several areas, circulation patterns (in and away from the

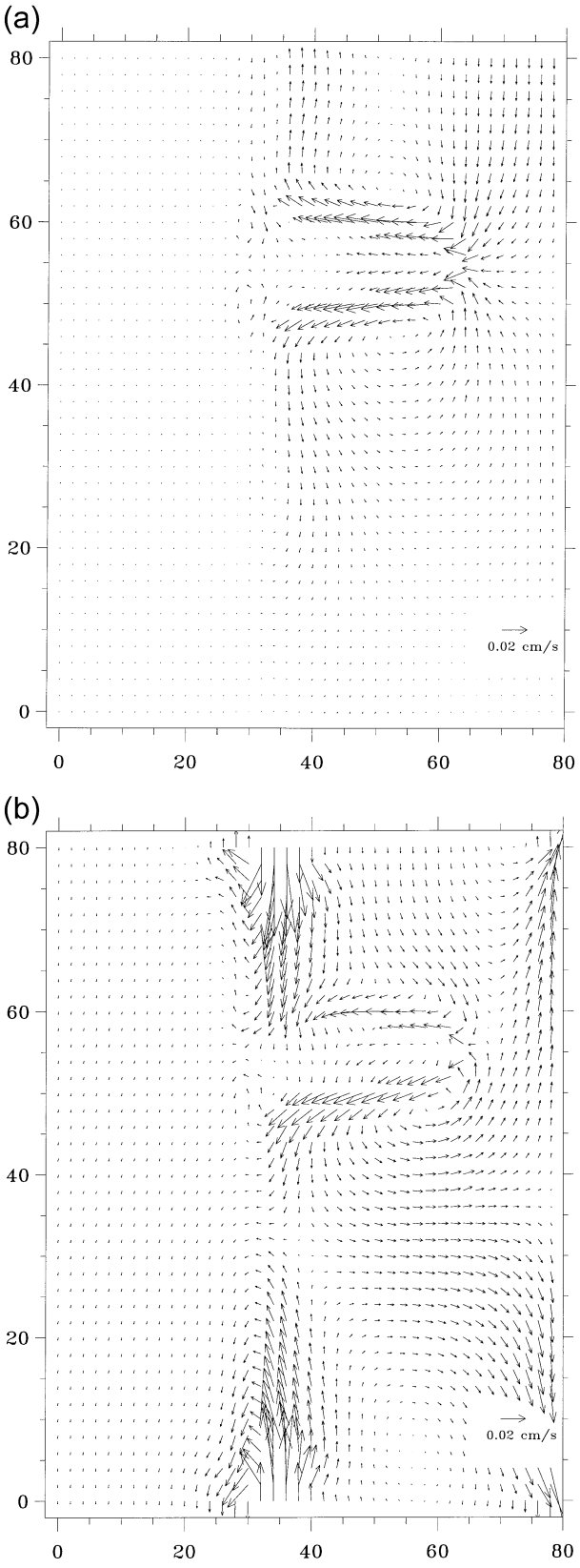

canyon), vertical velocities at the level of the canyon rim, and cross sections of meridional flow are compared. Reasons for the differences are shown as well as their impact on the circulation in the canyon.

There are several differences between the various simulations. The primary difference between the MO simulations and the other three is that a meridional pressure gradient is set up against the wind, which leads to slower surface currents and deep undercurrents away from the shelf. The most significant difference between the periodic case and the open boundary simulations is the strong flow variability that develops in the periodic case (due to energy being trapped in the model domain) that eventually degrades the solution. The simulations using the local solution OBC (FLR and FRS) are generally very similar (in most cases only the FLR solution will be shown).

Now the question arises: To what should one compare the results? We do not know of any appropriate analytical solution. The periodic case cannot be considered the ''truth'' due to the meridional variability in the topography. An extended domain, closed boundary case cannot be created because wind forcing exists everywhere, which will create an alongshore pressure gradient. Limiting the extent of the wind in an extended domain simulation creates a different dynamical situation because CTW will propagate across the wind band and establish an alongshore pressure gradient (Suginohara 1982; McCreary and Chao 1985). Stretched grids also affect the solution in subtle ways: a wave that propagates on an increasingly coarse grid becomes partially reflected up to the point where it can no longer be resolved and therefore it is then totally reflected (Haidvogel and Beckmann 1999).

However, in order to have some kind of control experiment, a simulation was created using a stretched grid with a resolution ranging from 500 m in an 80 km by 80 km region right around the canyon as before to as much as 10.5 km at the edge of the model domain. The number of grid points was increased in both directions resulting in a greatly expanded grid with a cross-shore distance of 1360 km and an alongshore distance of 2140 km (still with a constant f). This domain is large enough to prohibit any advected wrap-around effects in a periodic simulation by the time of the comparisons below (would require a flow of >2 m s^{-1}) and should limit most internal waves. An experiment (EXP) was performed by applying uniform upwelling winds over the entire extended model domain, which was periodic in the alongshore direction. This control experiment will not be a perfect analog of the the theoretical ''infinite''

←

FIG. 3. (a) Barotropic 2D flow in the reduced physics simulation at $t = 1$ day for the case with no sponge. (b) Barotropic flow in the reduced physics simulation at $t = 1$ day for the case with a sponge.

coast we are trying to mimic, but it can be a useful comparison.

a. Upwelling winds

Although there are no analytical solutions to this problem, enough similar numerical experiments have been done so that one can have at least a qualitative expectation of what the flow should look like. For upwelling winds, Ekman transport pulls water away from the coast setting up a cross-shelf surface height gradient that, due to geostrophy, forces a general flow along the coast in the direction of the wind. Depending on the geometry of the canyon and the vertical stratification of the water column, the canyon forces some of the water across bathymetry toward the coast. There also may or may not be a closed cyclonic circulation within (or even above) the canyon itself. Nevertheless, the canyon does not greatly change the general flow in the direction of the wind along the bathymetry well away from the canyon. Our initial simulations with open boundaries and upwelling winds all developed a small northward return flow along the SE corner of the model domain. When this flow was combined with dense water being upwelled out of the canyon onto the shelf (the problem did not happen with downwelling winds or with the model domain greatly expanded in the southern direction) an eddy formed on the shelf that propagated to the southern open boundary eventually resulting in an even larger return flow along much of the shelf. This problem vanished when the coastal depth was reduced from 50 to 5 m. Pathological flows form in models of estuarine plumes when the coastal depth was larger than twice the Ekman depth (Garvine 2001), due to a wall trapped baroclinic gravity wave.

There is a significant difference in the total alongshore volume transport for the upwelling wind cases, especially for the MO simulation (Fig. 4). The two cases that use the local solution of the barotropic flow have almost identical shelf transport, while the MO transport is closer to the periodic. The periodic case has considerably more southerly flow above the shelf break over the abyss than any of the open cases, which all have similar upper-layer transport. Below the shelf break, the total flow is strongly southward and nearly the same for all cases, except for MO, which is slightly northward. The extended domain periodic case has even more southerly transport above the shelf break than the base periodic case but has similar deep flow as all the other simulations except MO.

The current at 150 m at day 12 (Fig. 5) is generally weaker over the abyss for MO than the other three cases and a little stronger along the slope (and perhaps in the mouth of the canyon) for the periodic case than the open boundary simulations. Still, the general pattern is the same for all four simulations (so much so for FLR and FRS that only one is shown) and the cyclone in the canyon is almost identical in every instance.

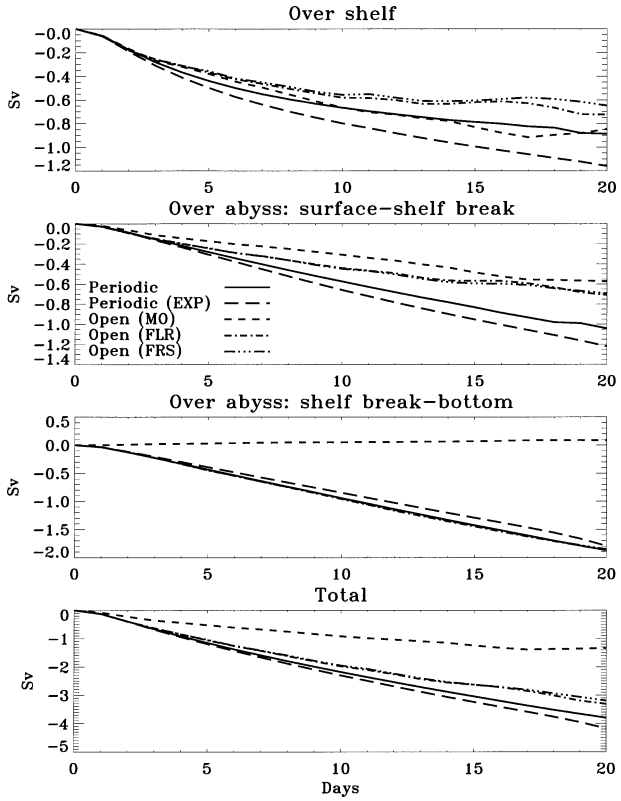

FIG. 4. Meridional (alongshore) volume transport in Sv (Sv $\equiv 10^6$ $m^3\ s^{-1}$): upwelling winds. The transport is calculated across a section at $y = 30$ km (see Fig. 2) or at the same position relative to the canyon (for the extended domain).

At 400 m at day 12 (Fig. 6), the MO flow is almost stopped (slightly northward) compared to the other three simulations. The flow at the mouth of the canyon at 400 m is the same for all but MO and is very small.

A zonal cross section of the meridional velocity through the middle of the canyon and out into the abyss (Fig. 7) shows the structure of the flow in all four cases looks similar. A cyclone is present in the upper canyon for all of the simulations; cases FLR and FRS are again almost identical. The periodic circulation is moderately stronger everywhere. The MO currents are weaker over the abyss and a deep countercurrent occurs against the wind. A cross section (over the same area as shown in the small domain cases) of the EXP simulation looks very similar to the periodic case except that the flow near the surface is a little stronger.

Individual terms in the momentum budget show the cause for the different solutions (Fig. 8). The principal difference among solutions is in the free surface slope and the resulting pressure gradient. The periodic model cannot develop a net alongshore surface pressure gradient while the open boundary cases may. There is a distinct difference between MO and the other cases that will be illustrated.

Several momentum terms are displayed at 400-m

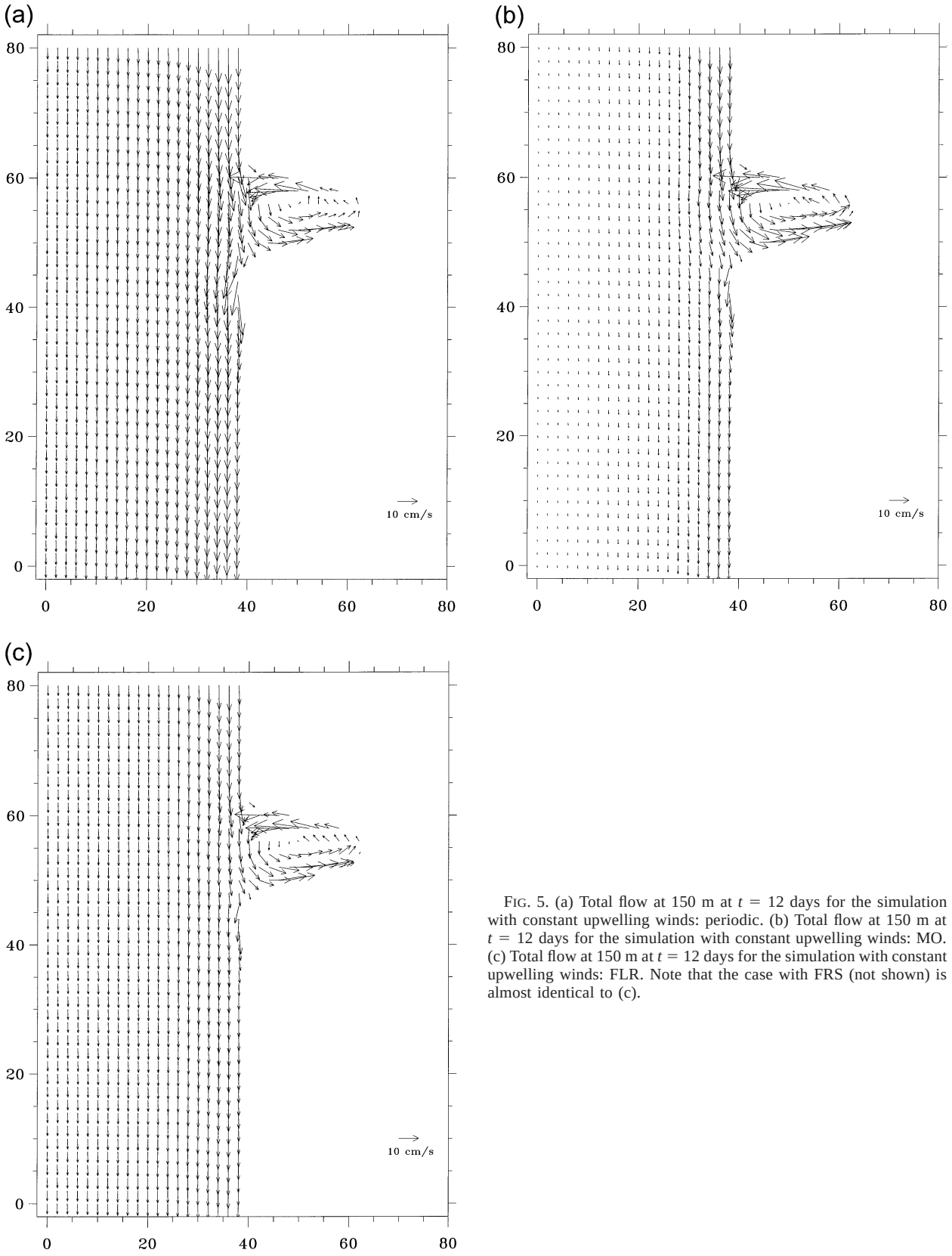

FIG. 5. (a) Total flow at 150 m at $t = 12$ days for the simulation with constant upwelling winds: periodic. (b) Total flow at 150 m at $t = 12$ days for the simulation with constant upwelling winds: MO. (c) Total flow at 150 m at $t = 12$ days for the simulation with constant upwelling winds: FLR. Note that the case with FRS (not shown) is almost identical to (c).

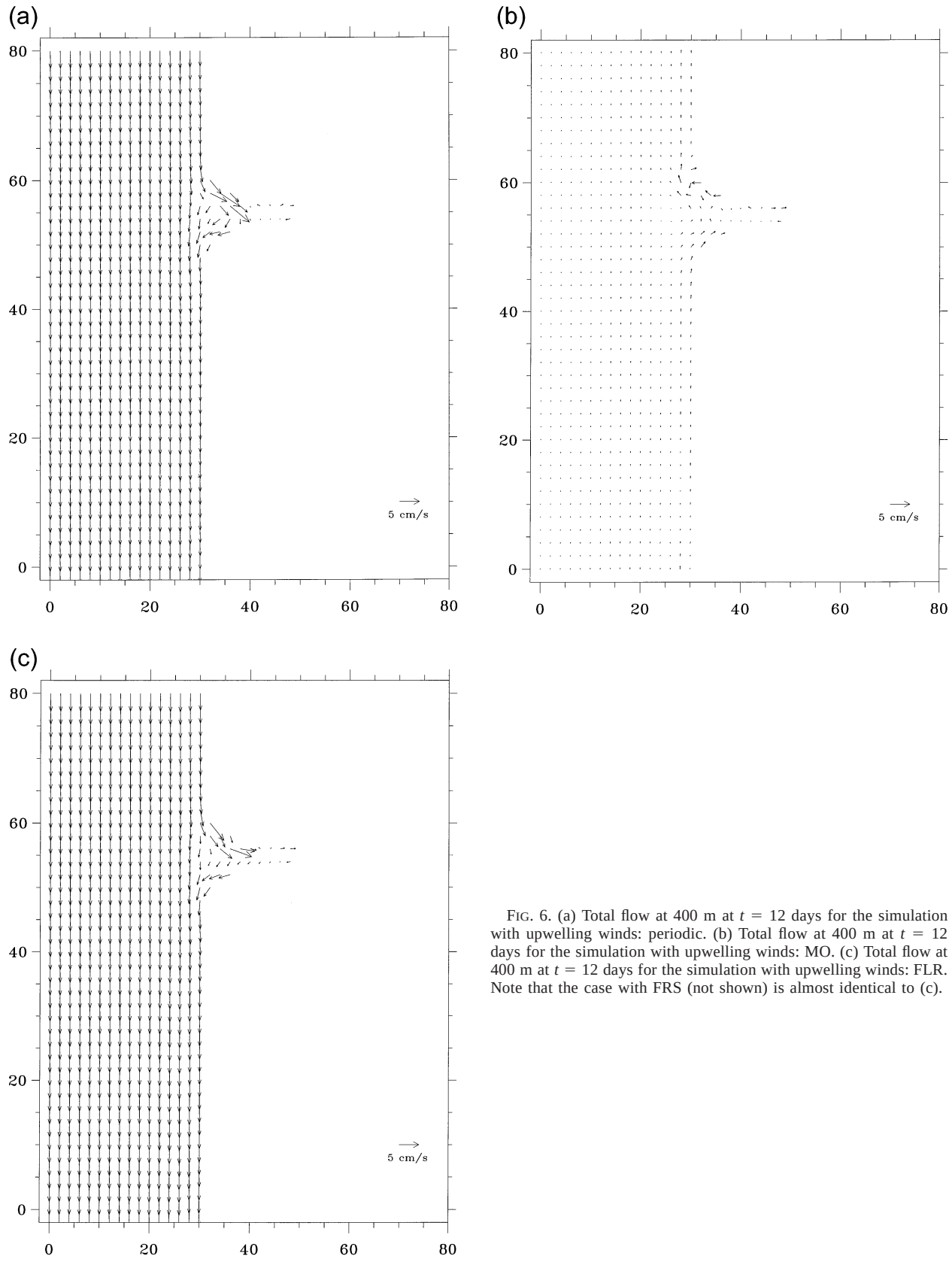

FIG. 6. (a) Total flow at 400 m at $t = 12$ days for the simulation with upwelling winds: periodic. (b) Total flow at 400 m at $t = 12$ days for the simulation with upwelling winds: MO. (c) Total flow at 400 m at $t = 12$ days for the simulation with upwelling winds: FLR. Note that the case with FRS (not shown) is almost identical to (c).

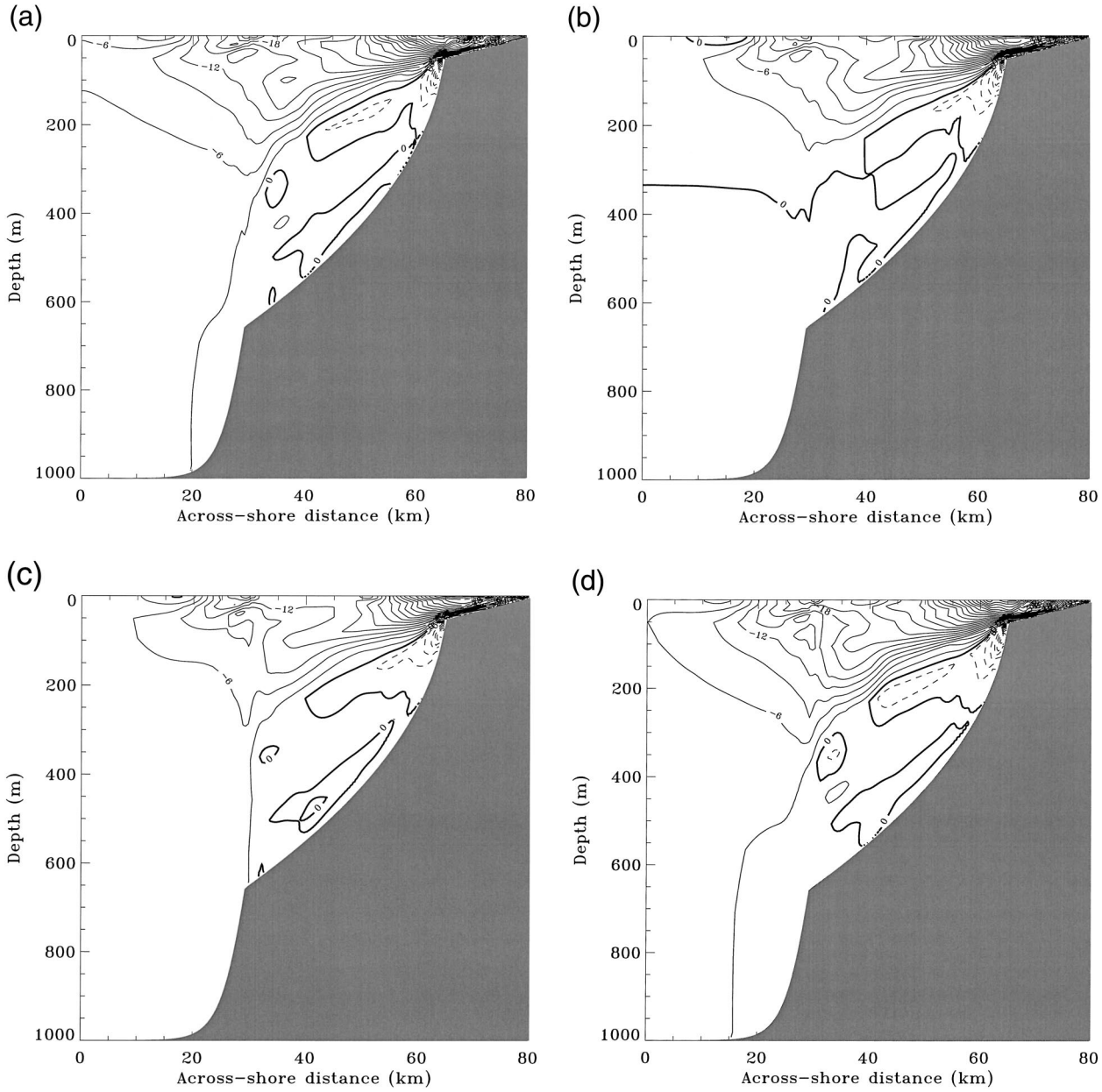

FIG. 7. (a) Zonal cross section through the center of the canyon of total alongshore velocity at $t = 12$ days for the simulation with upwelling winds: periodic case. The contour interval is 3 cm s^{-1} and velocities in the direction of the wind (<0) are drawn with solid lines. (b) As in (a) but for the MO simulation. (c) As in (a) but for the FLR simulation. Again, note that the case with FRS (not shown) is almost identical to (c). (d) As in (a) but for the EXP simulation.

depth after 1 day of wind forcing. The major terms are the pressure gradient and the Coriolis acceleration, which approximately cancel (Fig. 8, top 2 panels). However, MO has a clear positive pressure gradient [similar to results in a barotropic model by Palma and Matano (1998)], while the other cases (illustrated by the FLR solution) have gradients that change sign in different regions. Interestingly, the baroclinic pressure gradient, due to the density variations above 400 m, is largely compensated by the distortions of the free surface (Fig. 8, middle 2 panels). Off the shelf, the sea surface slope is clearly large for MO (sloping up to the south) but small for FLR.

The net meridional ageostrophic force (Fig. 8, lower-left panel) is southward (about 6×10^{-3} m^3 s^{-2}) for FLR (as well as FRS and periodic, figures not shown) but is mainly northward and more variable for MO. The total force due to the largest four terms (pressure gradient, Coriolis, horizontal advection, and vertical advection) is very close to the sum of the pressure gradient

and Coriolis terms indicating 1) the small contribution of the other forces and 2) the presence of an acceleration in the alongshore flow at this depth. Further, the net pressure force in MO indicates the importance of wave dynamics in the domain compared to the FLR case (Fig. 8, bottom-left panel).

How do these differences affect the conditions in the canyon? The structure of the upwelling at the level of the canyon rim/shelf break (150 m) looks quite similar among all four cases with downwelling over most of the north portion of the canyon and upwelling over the south after the cyclone is spun up. However, the magnitude of the maximum vertical velocity is somewhat stronger in the periodic simulation than in the three open boundary cases at 150 m, and there is more upwelling for the periodic case further down in the canyon (not shown). Consequently, the density surfaces are elevated more in the periodic case leading to cooler temperatures at 150 m (Fig. 9). In the upper part of the canyon the difference in the circulation is very slight.

Looking at the zonal momentum balance at 150 m (not shown), the periodic simulation has a stronger barotropic alongshore flow than the other simulations and thus geostrophy sets a higher cross-shore surface height. Yet this is balanced by a stronger Coriolis acceleration across the mouth of the canyon and a larger baroclinic pressure gradient force (pgf) across the interior (due to the stronger upwelling). The circulation in the deeper part of the canyon away from the mouth does not seem to be changed much at all by the different boundary conditions.

b. Downwelling winds

For the downwelling winds, Ekman transport now pushes water toward the coast resulting in a cross-shelf surface height gradient that forces a general flow along the coast in the direction of the wind. The canyon will again have an impact on the circulation, although not necessarily the inverse of the effect on upwelling flow (e.g., Klinck 1996).

Just as for the upwelling wind cases, there is a significant difference in the total alongshore volume transport for the downwelling wind cases (Fig. 10). Over the shelf, the periodic case has the largest alongshore transport, with MO and FLR nearly the same but less than the periodic. FRS has the smallest transport. Over the abyss, the periodic case again has more northward transport (both above and below the shelf break) than the others, while MO actually has a net slight southward countercurrent below the shelf break. The total transport is least for MO and greatest for the periodic case.

At 150 m on day 12, the MO flow is again weaker over the abyss than the other cases while the periodic flow is stronger along the slope and across the mouth of the canyon (Fig. 11). The strong anticyclone that extends almost to the head of the canyon is similar (away from the canyon mouth) for all four cases.

At 400 m (not shown), the MO flow over most of the abyss is a weak southward countercurrent while the other simulations have a stronger northward flow. Along the slope and across the mouth of the canyon, the periodic flow is strongly northward while the MO flow is southward and the FLR and FRS currents are nearly stationary. The flow in the canyon is very weak for all the cases. Even though the open boundary cases have different flow across the mouth of the canyon at this depth, the pattern in the canyon (a weak anticyclone) is the same. Later in the simulation (not shown) the pattern in the head of the canyon is still similar, but the pattern in midcanyon differs somewhat.

A momentum term balance (not shown) indicates that the horizontal advection terms are important enough at this time to change the circulation in midcanyon due to different flow past the mouth of the canyon. A zonal cross section of the meridional flow through the middle of the canyon and out into the abyss (not shown) shows an undercurrent against the wind across the abyss for MO. This is due to a net meridional change in surface elevation for the MO case (higher surface elevation to the north for the downwelling winds here) again creating a meridional pressure gradient acting in the opposite direction of the wind stress.

4. Discussion

The primary differences between the MO simulation and the other three are due to the meridional free surface pressure gradient against the wind forcing that is set up with these boundary conditions. The undercurrent forced by this pressure gradient is not unreasonable; there are many observations of undercurrents in coastal regions with upwelling winds (Neshyba et al. 1989) and some observations of undercurrents in regions with at least seasonal downwelling winds such as off the coast of Oregon and Washington (Hickey 1989) and the Leeuwin Current off the west coast of Australia (Church et al. 1989). There have also been several numerical simulations of the coastal ocean without a canyon, but with a similar continental slope/shelf bathymetry that produce an undercurrent. McCreary and Chao (1985) used a three-dimensional linear, continuously stratified and viscid semianalytical model (that assumed the alongshore flow was in geostrophic balance) stretching from 20° to 60°N with upwelling winds over the southern 20°. Many of their solutions did have a coastal undercurrent below the wind field (depending on such things as the shelf depth or the strength of vertical mixing). Middleton and Cirano (1999) used a primitive equation sigma coordinate model on an f plane with constant winds over a portion of their domain (4000 km in the alongshore direction) to study downwelling slope currents in the Great Australian Bight. In their simulations, an undercurrent does exist and they determined that it could be due to linear CTW dynamics for the first 10–

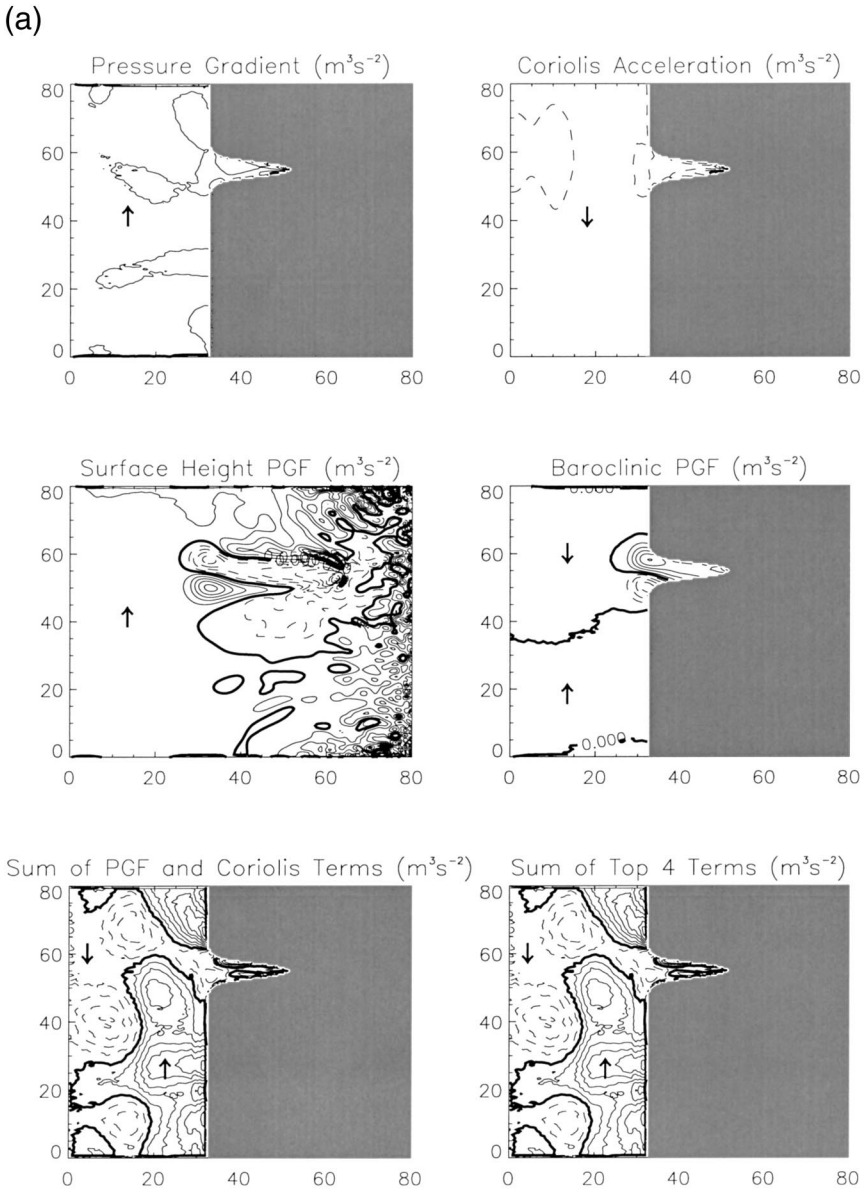

FIG. 8. (a) Meridional momentum balance terms at 400 m at $t = 1$ day for the simulation with upwelling winds: MO case. The units are $m^3\ s^{-2}$ and must be divided by the model grid box area in order to represent an actual acceleration. The contour intervals are $10^{-2}\ m^3\ s^{-2}$ for the top two panels, $2.5 \times 10^{-2}\ m^3\ s^{-2}$ for the middle two panels, and $1.5 \times 10^{-3}\ m^3\ s^{-2}$ for the bottom two. The arrow represents the direction of the plotted term at that location.

20 days but afterward is driven by an alongshore pressure gradient due to sea level.

This raises the following question: Are the simulated open boundaries causing errors that lead to an erroneous surface height gradient? Two-dimensional (no alongshore dimension) simulations of the coastal current under upwelling (Allen et al. 1995) or downwelling (Allen and Newberger 1996) winds do not create an undercurrent. Both the McCreary and Chao model and the Middleton and Cirano model had wind forcing over only part of the model domain. In both cases, CTW propagate across the area of wind forcing in a timescale on the order of tens of days and establish an alongshore pressure gradient. In our model, the wind stress was constant over the entire domain and no external surface height gradient was imposed. In fact, the only thing that varied in the alongshore direction was the topography. Model simulations using a constant alongshore bathymetry (no canyon) showed only a slight change in the undercurrent even though with a constant wind field this model is then, in effect, two-dimensional. As we can think of no physical reason for an undercurrent to exist in this sit-

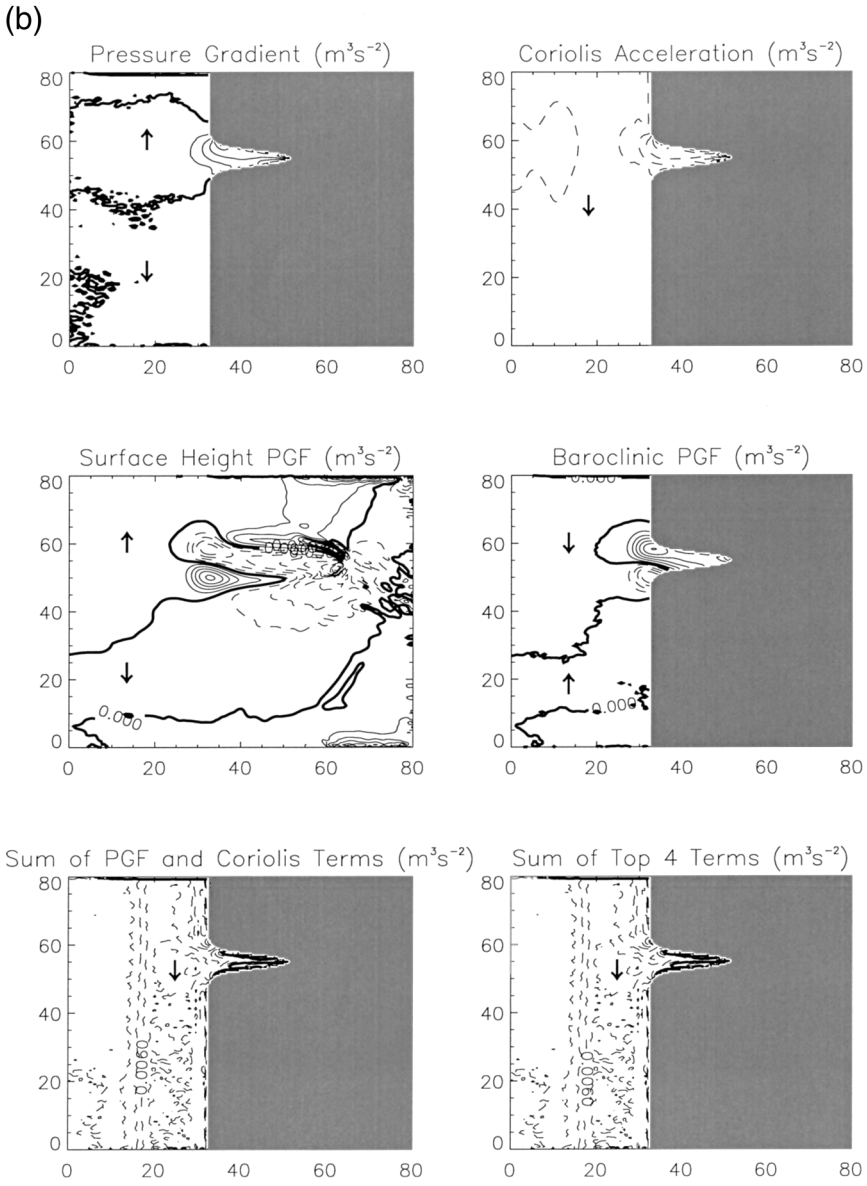

FIG. 8. (b) As in (a) but for the FLR simulation.

uation, we conclude that the alongshore surface height gradient is due to an error caused by the MO boundary conditions. As mentioned previously, others have found similar problems using MO on barotropic coastal models (Røed and Cooper 1987; Palma and Matano 1998).

There are other differences between the periodic case and the open boundary cases. The periodic flow is generally a little faster (especially the EXP case) with small differences in the density structure in the canyon. However, the primary difference, at least for the upwelling winds, is the stability of the solution. The presence of the canyon creates a disturbance in the barotropic flow that, for the periodic case, grows as it is not allowed to advect or propagate out of the model domain. After several days, waves in the surface height are visibly traveling southward in the alongshore direction and continue to grow well past the point where they are affecting the model flow (Fig. 12). A similar problem occurs with downwelling winds (not shown) but not to the same extent.

Periodic model domains have additional problems with the variation of the Coriolis parameter (β plane). For small alongshore distances, β effects are weak, but some energy loss from the coast does occur by Rossby waves and investigating these effects requires open model domains. We attempted some simulations in a periodic domain with a variable Coriolis parameter without undue difficulty and with similar results to the f-plane cases. However, these simulations extended only a few weeks and were in a rather short domain (80 km).

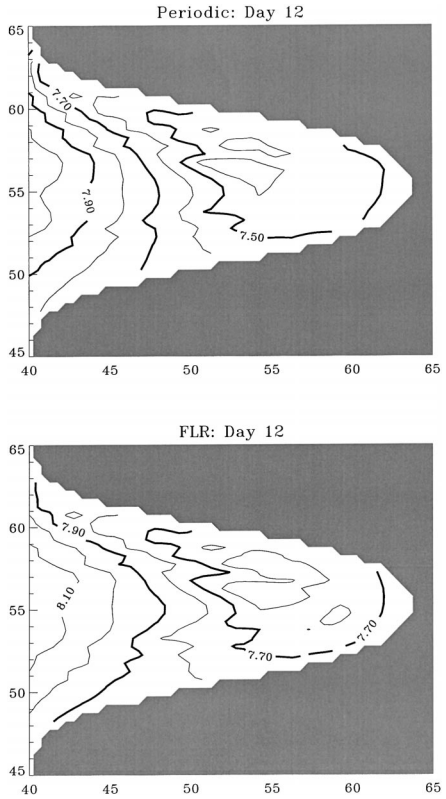

FIG. 9. Temperature (°C) in the canyon at 150 m for $t = 12$ days for the simulation with upwelling winds for the periodic and FLR cases. The contour interval is 0.10°C.

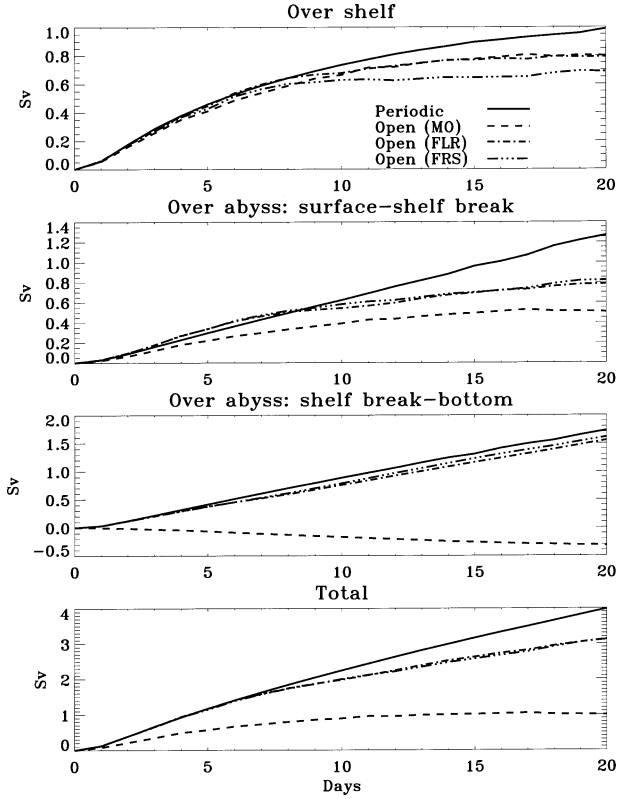

FIG. 10. Meridional (alongshore) volume transport in Sv: downwelling winds. The transport is calculated across a section at $y = 30$ km (see Fig. 2).

There is not a great deal of difference between the FLR and FRS results presented here. The alongshore transport above the shelf break in the FRS case with downwelling winds is lower than the other open boundary cases when compared to the periodic flow (Fig. 10). The presence of the canyon in the bathymetry prevents us from using the regular domain periodic case as a benchmark as was done by Palma and Matano (1998), although an extended periodic domain may be used as one that would argue slightly in favor of the FLR solution. Since we know of no analytical solution for the fully nonlinear case, it is hard to determine which is a better solution to the open boundaries. Recently, simulations have been run using the same three open OBCs on a more realistic and rugged model topography consisting of the area around Astoria Canyon (B. Hickey et al. 2002, unpublished manuscript). The MO simulation still had an undercurrent against the wind across most of the abyss while the FLR and FRS cases did not.

5. Conclusions

The different boundary conditions have a noticeable impact on the general circulation of the model. Ideally, we would have observations, an analytical solution, or results from a larger model domain near the boundaries of our model domain so that we could impose the correct boundary conditions but that is unlikely for this problem. Instead we are forced to choose values on the boundaries that are either assumed or extrapolated from the interior values and will hopefully approximate the circulation in the real ocean. This paper came about not out of a desire to exhaustively compare different passive OBCs, but from an attempt to find one that was easy to implement and would work well for our studies on circulation in submarine canyons. Many different OBCs were tried on a primitive equation coastal ocean model with variable alongshore bathymetry, but only a few of the tested sets appeared to be stable. The specific boundary condition that had the most impact on the simulations was the alongshore barotropic flow and the three solutions varied only in that aspect—either modified Orlanski (MO), Flather conditions combined with a local solution approach (FLR) or a flow relaxation scheme (FRS) where the prescribed value on the boundary is the local solution. Unfortunately, these results are probably only representative for similarly scaled models. When we used the same model code, but for a different coastal ocean setup (west of the Antarctic Peninsula) with much coarser grid resolution (5 km vs 500 km) and stronger external forcing (the Antarctic Circumpolar Current goes through our domain), we were forced to

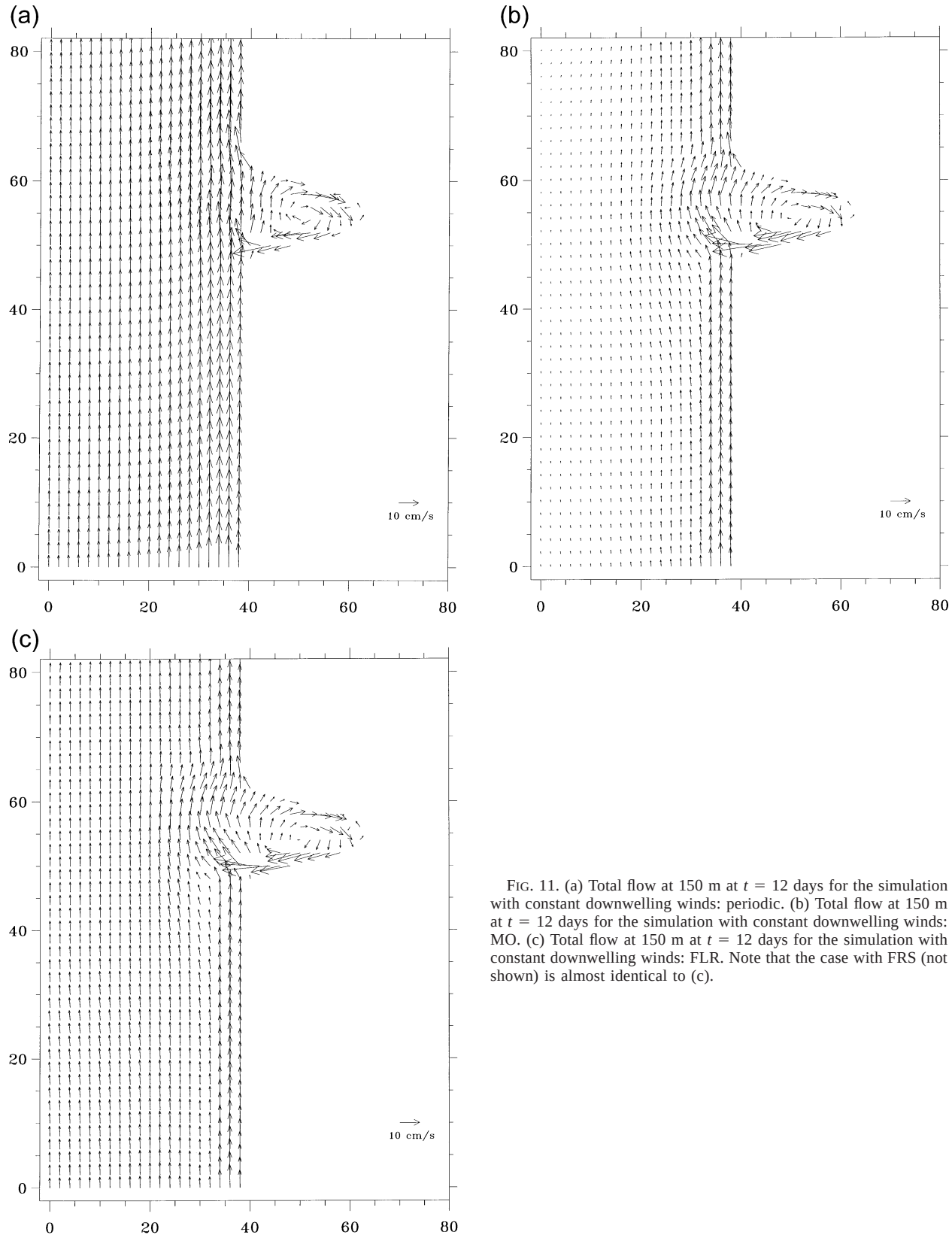

FIG. 11. (a) Total flow at 150 m at $t = 12$ days for the simulation with constant downwelling winds: periodic. (b) Total flow at 150 m at $t = 12$ days for the simulation with constant downwelling winds: MO. (c) Total flow at 150 m at $t = 12$ days for the simulation with constant downwelling winds: FLR. Note that the case with FRS (not shown) is almost identical to (c).

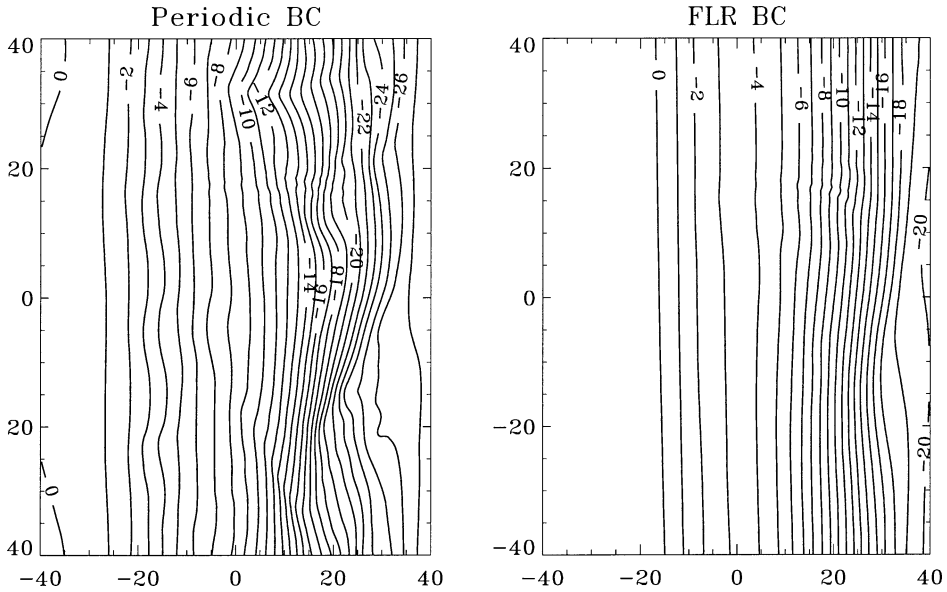

FIG. 12. Model surface height at $t = 20$ d: upwelling winds.

use sponge layers, volume conservation, and two-dimensional radiation [setup similar to Marchesiello et al. (2001)].

The choice of an OBC affects the flow in the alongshore direction. The differences in the current past the mouth of the canyon do change the circulation in the canyon itself. The strong upwelling out of the canyon (one of the most important effects of submarine canyons on the general coastal circulation) is quite similar in pattern but can have different magnitudes due to the difference in forcing from the varying strength of the flow past the canyon. This led to a difference in the density structure in the upper canyon. The strength of the cyclone in the upper canyon, and the momentum balance that creates it, varied little among the cases. However, the relative strengths of the different terms did vary with stronger height gradients being offset by stronger density gradients. The circulation in the interior of the deep canyon did not differ much initially even though the flow outside the canyon could sometimes be in opposite directions. However, the nonlinear momentum terms eventually become important and the difference in the flow past the entrance of the canyon does impact the circulation further in the interior.

Of these three stable OBCs, the MO boundary conditions created a false (we believe) alongshore surface height gradient that led to an undercurrent and greatly changed the alongshore transport. The periodic boundary conditions proved to be unsuitable for extended simulations, especially with the upwelling winds, due to propagating disturbances that were not allowed to leave the model domain. There was not much difference between the FLR and FRS conditions for the simulations tested here. A set of OBCs similar to FRS (at least for the velocities) was also tested extensively for a fully barotropic coastal ocean model by Palma and Matano (2000) and was found to be their preferred solution with another set similar to FLR their second choice. For all these reasons, we use both FLR and FRS for our modeling studies.

Acknowledgments. We would like to thank Drs. Glen Wheless and Cathy Lascara of the Virtual Environment Lab at the Commonwealth Center for Coastal Physical Oceanography who provided time on the SGI Origin 2000 (made available with funding provided through NSF Grant OCE-98-71100 as well as from Old Dominion University) that these simulations were run on. Dr. Hernan Arango provided us with the Beta 1.0 release of ROMS. Dr. Richard Garvine suggested using the shallower coastal wall. Helpful discussions with Drs. Susan Allen, Barbara Hickey, and Dale Haidvogel as well as the comments of the three anonymous reviewers contributed greatly to this work. This work was supported by the U.S. National Science Foundation through Grant OCE-96 18239. Computer facilities and support were provided by the Commonwealth Center for Coastal Physical Oceanography.

REFERENCES

Allen, J. S., and P. A. Newberger, 1996: Downwelling circulation on the Oregon continental shelf. Part I: Response to idealized forcing. *J. Phys. Oceanogr.*, **26,** 2011–2035.

——, P. A. Newberger, and J. Federiuk, 1995: Upwelling circulation on the Oregon continental shelf. Part I: Response to idealized forcing. *J. Phys. Oceanogr.*, **25,** 1843–1866.

Allen, S. E., 1996: Topographically generated, subinertial flows within a finite length canyon. *J. Phys. Oceanogr.*, **26,** 1608–1632.

Ardhuin, F., J.-M. Pinot, and J. Tintoré, 1999: Numerical study of the circulation in a steep canyon off the Catalan coast (western Mediterranean). *J. Geophys. Res.*, **104,** 11 115–11 135.

Bennett, A. F., and P. E. Kloeden, 1978: Boundary conditions for limited-area forecasts. *J. Atmos. Sci.,* **35,** 355–375.

Camerlengo, A. L., and J. J. O'Brien, 1980: Open boundary conditions in rotating fluids. *J. Comput. Phys.,* **35,** 12–35.

Cannon, G. A., R. K. Reed, and P. E. Pullen, 1985: Comparison of El Niño events off the Pacific Northwest. *El Niño North: Niño Effects in the Eastern Subartic Pacific Ocean,* W. S. Wooster and D. L. Fluharty, Eds., Washington Sea Grant Program, 75–84.

Chapman, D. C., 1985: Numerical treatment of cross-shelf open boundaries in a barotropic coastal ocean model. *J. Phys. Oceanogr.,* **15,** 1060–1075.

Church, J. A., G. R. Cresswell, and J. S. Godfrey, 1989: The Leeuwin Current. *Poleward Flows along Eastern Ocean Boundaries,* S. J. Neshyba et al., Eds., Coastal and Estuarine Studies, Vol. 34, Springer-Verlag, 230–254.

Csanady, G. T., 1988: Ocean currents over the continental slope. *Advances in Geophysics,* Vol. 30, Academic Press, 95–203.

Flather, R. A., 1976: A tidal model of the northwest European continental shelf. *Mem. Soc. Roy. Sci. Liege, Ser. 6,* **10,** 141–164.

Garvine, R. W., 2001: The impact of model configuration in studies of buoyant coastal discharge. *J. Mar. Res.,* **59,** 193–225.

Haidvogel, D. B., and A. Beckmann, 1998: Numerical models of the coastal ocean. *The Sea,* K. H. Brink and A. R. Robinson, Eds., the Global Coastal Ocean, Vol. 10, John Wiley and Sons, 457–482.

——, and ——, 1999: *Numerical Ocean Circulation Modeling.* Series on Environmental Science and Management, Vol. 2, Imperial College Press, 319 pp.

Hedström, K. S., 1997: (DRAFT) User's manual for an S-Coordinate Primitive Equation Ocean Circulation Model (SCRUM) Version 3.0. Institute of Marine and Coastal Sciences, Rutgers University Contribution 97-10, 116 pp.

Hickey, B., 1989: Poleward flow near the northern and southern boundaries of the U.S. West Coast. *Poleward Flows along Eastern Ocean Boundaries,* S. J. Neshyba et al., Eds., Coastal and Estuarine Studies, Vol. 34, Springer-Verlag, 160–175.

——, 1995: Coastal submarine canyons. *Topographic Interactions in the Ocean: Proc. 'Aha Huliko' a Hawaiian Winter Workshop,* Honolulu, HI, University of Hawaii at Manoa, 95–110.

——, 1997: The response of a steep-sided, narrow canyon to time-variable wind forcing. *J. Phys. Oceanogr.,* **27,** 697–726.

Huthnance, J. M., 1992: Extensive slope currents and the ocean-shelf boundary. *Progress in Oceanography,* Vol. 29, Pergamon, 161–196.

——, L. A. Mysak, and D.-P. Wang, 1986: Coastal trapped waves. *Baroclinic Processes on Continental Shelves,* C. N. K. Mooers, Ed., Coastal and Estuarine Series, Vol. 3, Amer. Geophys. Union, 1–18.

Jensen, T. G., 1998: Open boundary conditions in stratified ocean models. *J. Mar. Sys.,* **16,** 297–322.

Klinck, J. M., 1988: The influence of a narrow transverse canyon on initially geostrophic flow. *J. Geophys. Res.,* **93,** 509–515.

——, 1996: Circulation near submarine canyons: A modeling study. *J. Geophys. Res.,* **101,** 1211–1223.

Large, W. G., J. C. McWilliams, and S. C. Doney, 1994: Oceanic vertical mixing: A review and model with a nonlocal boundary layer parameterization. *Rev. Geophys.,* **32,** 363–403.

Marchesiello, P., J. C. McWilliams, and A. Shchepetkin, 2001: Open boundary condition for long-term integration of regional oceanic models. *Ocean Modell.,* **3,** 1–20.

Martinsen, E. H., and H. Engedahl, 1987: Implementation and testing of a lateral boundary scheme as an open boundary condition in a barotropic ocean model. *Coastal Eng.,* **11,** 603–627.

McCreary, J. P., and S.-Y. Chao, 1985: Three-dimensional shelf circulation along an eastern ocean boundary. *J. Mar. Res.,* **43,** 13–36.

Middleton, J. F., and M. Cirano, 1999: Wind-forced downwelling slope currents: A numerical study. *J. Phys. Oceanogr.,* **29,** 1723–1743.

Neshyba, S. J., C. N. K. Mooers, R. L. Smith, and R. T. Barber, Eds.,1989: *Poleward Flows along Eastern Ocean Boundaries.* Coastal and Estuarine Studies, Vol. 34, Springer-Verlag, 374 pp.

Oliger, J., and A. Sündstrom, 1978: Theoretical and practical aspects of some initial boundary value problems in fluid dynamics. *SIAM J. Appl. Math.,* **35,** 419–446.

Orlanski, I., 1976: A simple boundary condition for unbounded hyperbolic flows. *J. Comput. Phys.,* **21,** 251–269.

Palma, E. D., and R. P. Matano, 1998: On the implementation of passive open boundary conditions for a general circulation model: The barotropic mode. *J. Geophys. Res.,* **103,** 1319–1341.

——, and ——, 2000: On the implementation of open boundary conditions for a general circulation model: The three-dimensional case. *J. Geophys. Res.,* **105,** 8605–8627.

Pérenne, N., J. Verron, D. Renouard, D. L. Boyer, and X. Zhang, 1997: Rectified barotropic flow over a submarine canyon. *J. Phys. Oceanogr.,* **27,** 1868–1893.

Raymond, W. H., and H. L. Kuo, 1984: A radiation boundary condition for multi-dimensional flows. *Quart. J. Roy. Meteor., Soc.,* **110,** 535–551.

Reed, R. K., 1984: Oceanographic conditions off the Pacific Northwest following the 1982 El Niño event. *Mar. Fish. Rev.,* **46,** 7–12.

Røed, L. P., and O. M. Smedstad, 1984: Open boundary conditions for forced waves in a rotating fluid. *SIAM J. Sci. Stat. Comput.,* **5,** 414–426.

——, and C. Cooper, 1987: A study of various open boundary conditions for wind-forced barotropic numerical models. *Three-dimensional Models of Marine and Estuarine Dynamics,* J. C. J. Nihoul and B. N. Jamart, Eds., Elsevier, 305–335.

She, J., and J. M. Klinck, 2000: Flow near submarine canyons driven by constant winds. *J. Geophys. Res.,* **105,** 28 671–28 694.

Suginohara, N., 1982: Coastal upwelling: Onshore–offshore circulation, equatorward coastal jet and poleward undercurrent over a continental shelf-slope. *J. Phys. Oceanogr.,* **12,** 272–284.

Wilkin, J. L., 1987: A computer program for calculating frequencies and modal structures of free coastal-trapped waves. Tech. Rep. WHOI 87-53, Woods Hole Oceanographic Institute, Woods Hole, MA, 50 pp.